Experimental Investigation of Coil Curvature Effect on Heat Transfer and Pressure Drop Characteristics of Shell and Coil Heat Exchanger

ARTICLE · OCTOBER 2014

DOI: 10.1115/1.4028612

4 AUTHORS:

Mohamed Reda Salem
Benha University
3 PUBLICATIONS **0** CITATIONS
SEE PROFILE

Karam El-Shazly
Benha University
11 PUBLICATIONS **15** CITATIONS
SEE PROFILE

Ramadan Sakr
Benha University
19 PUBLICATIONS **8** CITATIONS
SEE PROFILE

Ragab Khalil Ali
Benha University
13 PUBLICATIONS **6** CITATIONS
SEE PROFILE

Experimental Investigation of Coil Curvature Effect on Heat Transfer and Pressure Drop Characteristics of Shell and Coil Heat Exchanger

M. R. Salem
Mechanical Engineering Department,
Faculty of Engineering at Shoubra,
Benha University,
108 Shoubra St.,
Cairo, Egypt
e-mail: me_mohamedreda@yahoo.com

K. M. Elshazly
Mechanical Engineering Department,
Faculty of Engineering at Shoubra,
Benha University,
108 Shoubra St.,
Cairo, Egypt
e-mail: drkaramelshazly@yahoo.com

R. Y. Sakr
Mechanical Engineering Department,
Faculty of Engineering at Shoubra,
Benha University,
108 Shoubra St.,
Cairo, Egypt
e-mail: rsakr85@yahoo.com

R. K. Ali
Mechanical Engineering Department,
Faculty of Engineering at Shoubra,
Benha University,
108 Shoubra St.,
Cairo, Egypt
e-mail: ragabkhalil1971@gmail.com

The present work experimentally investigates the characteristics of convective heat transfer in horizontal shell and coil heat exchangers in addition to friction factor for fully developed flow through the helically coiled tube (HCT). The majority of previous studies were performed on HCTs with isothermal and isoflux boundary conditions or shell and coil heat exchangers with small ranges of HCT configurations and fluid operating conditions. Here, five heat exchangers of counter-flow configuration were constructed with different HCT-curvature ratios (δ) and tested at different mass flow rates and inlet temperatures of the two sides of the heat exchangers. Totally, 295 test runs were performed from which the HCT-side and shell-side heat transfer coefficients were calculated. Results showed that the average Nusselt numbers of the two sides of the heat exchangers and the overall heat transfer coefficients increased by increasing coil curvature ratio. The average increase in the average Nusselt number is of 160.3–80.6% for the HCT side and of 224.3–92.6% for the shell side when δ increases from 0.0392 to 0.1194 within the investigated ranges of different parameters. Also, for the same flow rate in both heat exchanger sides, the effect of coil pitch and number of turns with the same coil torsion and tube length is remarkable on shell average Nusselt number while it is insignificant on HCT-average Nusselt number. In addition, a significant increase of 33.2–7.7% is obtained in the HCT-Fanning friction factor (f_c) when δ increases from 0.0392 to 0.1194. Correlations for the average Nusselt numbers for both heat exchanger sides and the HCT Fanning friction factor as a function of the investigated parameters are obtained.
[DOI: 10.1115/1.4028612]

Keywords: heat exchanger, experimental, helically coiled tube, curvature, friction

1 Introduction

In most of the industrial applications, increasing the thermal performance of heat exchangers affects directly on energy, material, and cost savings. The major challenge in designing heat exchangers is to make the equipment compact and achieve a high heat transfer rate with minimum pumping power [1]. Coiled tubes of helical shape are one of the enhancement techniques that are widely used as heat exchangers and have applications in various industries: chemical, biological, petrochemical, mechanical, biomedical, etc.

This wide use of HCTs is because they are compact and promote good mixing of the fluids that increase the heat transfer coefficients. In addition, this equipment is low cost and of easy construction and maintenance [2–16]. Due to the extensive application of the HCTs in these fields, knowledge about the heat transfer and pressure drop characteristics is very important.

Topakoglu [17] studied the flow pattern for steady incompressible viscous laminar flow in curved pipes. Results showed that the flow rate depends on two independent variables, Reynolds number and δ. McConalogue and Srivastava [18] performed numerical studies to determine the characteristics of the secondary flow for fully developed laminar flow. Their results showed that as the axial velocity increases, the maximum value of the axial velocity moves toward the outer wall and the secondary vortices migrate closer to the outer wall. Hüttl and Friedrich [19,20] numerically studied the effects of coil curvature and torsion, λ, on the characteristics of turbulent incompressible fluid flow in HCTs. They demonstrated that the effect of torsion on the axial velocity is much lower than the curvature effect but it could not be neglected. Gammack and Hydon [21] presented analytic and numerical solutions for flows in pipes with nonuniform curvature and torsion. They found that as δ increases, the axial velocity is forced toward the outer wall and the secondary velocity field is increased in strength. In addition, increasing torsion skews the components of velocity in the direction of increasing torsion. This was confirmed numerically by Masud et al. [22] for incompressible viscous steady flow through a curved pipe with circular cross section. Yu et al. [23] experimentally performed three-dimensional laser Doppler anemometry measurements on developed laminar flow in three HCTs ($0.0734 \le \delta \le 0.1374$ and $0.0793 \le \lambda \le 0.193$). The authors reported that δ and λ are the key parameters to affect the centrifugal force on fluid in a HCT.

There are several studies in the literature concerning the friction losses in HCTs. Eustice [24,25] experimentally noted an increase in resistance to flow for the curved tube compared to the straight tube and this increase in resistance could be correlated to δ. Dean [26] explained the higher pressure gradient in a curved pipe by that some of the fluid is in continual oscillation between the central part of the pipe, where the velocity is high, and the outer portion of the pipe, where the velocity is low. This movement is due to the centrifugal forces caused by the pipe curvature and results

Contributed by the Heat Transfer Division of ASME for publication in the Journal of Thermal Science and Engineering Applications. Manuscript received April 5, 2014; final manuscript received September 5, 2014; published online October 28, 2014. Assoc. Editor: Bengt Sunden.

in a loss of energy. White [27,28] experimentally studied the resistance of an isothermal flow of water and mineral oil through curved pipes. It was shown that, for $De < 11.6$, there is no difference in flow resistance compared to straight tubes.

Ito [29] performed experiments on smooth curved pipes with δ from 0.00154 to 0.061. Results showed that for turbulent flow, f_c, is equivalent to that of a straight pipe for values of $Re_t\ \delta^2$ below 0.034. A correlation was proposed for $0.034 < Re_t\ \delta^2 < 300$ and $15{,}000 < Re_t < 150{,}000$. Mori and Nakayama [30–32] theoretically studied the pressure drop in curved pipes with laminar and turbulent isothermal flow. A correlation was proposed for $13.5 < De < 2000$. Schmidt [33] studied the pressure drop for laminar flow inside HCTs for isothermal and nonisothermal flow conditions under constant wall temperature. The author concluded that the physical properties should be determined at the film temperature. The effect of δ and p_c on f_c for Newtonian fluids flowing through HCTs was studied by Mishra and Gupta [90]. Pressure drop data in the turbulent regions were reported and a correlation was obtained for $4500 < Re_t < 100{,}000$, $0.00289 < \delta < 0.1493$, and $0 < p_c/D_c < 25.4$.

Prasad et al. [34] experimentally studied the pressure drop in a HCT in shell heat exchanger. The experimental setup consisted of copper HCTs with δ of 0.0254 and 0.0575 for two separate tests. A correlation for f_c was developed for turbulent flow in the range of $Re_{cr} < Re_t < 59{,}500$. Ali [35] experimentally studied the pressure drop for steady isothermal flow of Newtonian fluids in HCTs. Generalized pressure drop correlations were developed in terms of the Euler and Reynolds numbers and geometrical group. Pimenta and Campos [36] determined f_c experimentally with simultaneous heat transfer for Newtonian and non-Newtonian fluids at constant wall temperature as boundary condition for fully developed laminar flow inside vertical HCT. It was concluded that f_c for non-Newtonian fluids was similar to those for Newtonian fluids when $De < 80$.

There is a significant amount of experimental and numerical studies in the literature regarding the convective heat transfer in isothermal and isoflux heated HCTs. Kirpikov [37] experimentally studied the heat transfer for turbulent flow of water in HCTs having δ of 0.1, 0.0769, and 0.0556. Heat transfer coefficients were obtained using the wall to bulk temperature difference and a correlation was proposed for the average Nusselt number of HCT flow ($\overline{Nu}$) for $10{,}000 < Re_t < 45{,}000$ and $Pr \approx 7$. Seban and McLaughlin [38] experimentally studied the heat transfer for oil laminar flow and water turbulent flow in uniformly heated HCTs ($0.0096 \le \delta \le 0.0588$). They concluded that the outer periphery has higher local Nusselt number than the inner with both being substantially higher than values for a straight pipe under the same conditions.

Experimental results for forced convection heat transfer for turbulent flow of water through steam heated coiled tubes were reported by Rogers and Mayhew [39]. Three coils with δ of 0.0926, 0.075, and 0.05 were used during experiments. They proposed a correlation for Re_t between 10,000 and 100,000. Theoretical and experimental studies on forced convective heat transfer in HCTs were carried out by Mori and Nakayama [30–32] with laminar and turbulent flow under isoflux and isothermal conditions. Results indicated that the heat transfer coefficient is improved by a factor related to De.

Numerical studies for uniform wall heat flux with peripherally uniform wall temperature, with $1 < De < 1200$, $0.005 < Pr < 1600$, and $0.01 < \delta < 0.1$, were performed by Kalb and Seader [40]. For $Pr > 0.7$, it was shown that the local Nusselt number in the area of the inner wall was always less than that of a straight tube. The local Nusselt number on the outer wall continued to increase with increasing De. Correlations were developed to estimate $\overline{Nu}$. Janssen and Hoogendoorn [41] studied experimentally and numerically the laminar convective heat transfer for both isoflux and isothermal heated HCTs. The effect of the different kinds of boundary conditions is shown to be small. Fully developed laminar flow and heat transfer was studied numerically by Zapryanov et al. [42]. Their work focused on the case of constant wall temperature and showed that $\overline{Nu}$ increased with increasing Pr, even for cases at the same De.

Xin and Ebadian [43] experimentally studied the effect of Pr and geometric parameters on the convective heat transfer characteristics in uniformly heated HCTs. Empirical correlations were proposed for the fully developed flow ($0.0267 < \delta < 0.0884$ and $0.0637 < \lambda < 0.8149$). Bai et al. [6] experimentally studied the turbulent heat transfer in horizontal HCTs under constant heat flux. They concluded that the local heat transfer coefficient on the outer wall could be 3–4 times that of the inner wall, and it is observed that $\overline{Nu}$ for horizontal HCT is less than that for vertical one for the same conditions. Prabhanjan et al. [44] compared experimentally the heat transfer coefficient for HCT versus straight tube heat exchangers. They found that the HCT had a heat transfer coefficient 1.16 and 1.43 times larger than for the straight tube heat exchanger for 40 and 50 °C, respectively.

Rennie and Raghavan [45,46] performed experimental and numerical studies on a double-pipe helical heat exchanger. Results showed that the overall heat transfer coefficients increase with higher inner Dean number. Jayakumar et al. [47] performed an experimental and numerical estimation of heat transfer in vertical shell and coil heat exchangers for turbulent regime ($2000 < De < 12{,}000$ and $1 < Pr < 3.5$). A correlation was proposed numerically and validated against experiments. Jayakumar et al. [48] numerically analyzed the characteristics of heat transfer under turbulent flow of water through HCTs for constant temperature and constant wall heat flux boundary conditions. Results showed that local Nusselt number on the outer side of the HCT is higher than that at the inner side. The authors developed correlations to estimate $\overline{Nu}$ for $14{,}000 < Re_t < 70{,}000$, $3000 < De < 22{,}000$, $3 < Pr < 5$, and $0.05 < \delta < 0.2$.

Shokouhmand et al. [49] carried out an experimental study of shell and coil heat exchangers using Wilson plots for both parallel and counter flow configurations. Salimpour [50,51] experimentally studied the heat transfer characteristics for laminar flow of oil and water inside HCT counter flow configuration. Empirical correlations were developed to predict the heat transfer coefficients of both fluids inside the HCT as a function of De, Pr, and λ. Purandare et al. [52] presented a comparative analysis of the different correlations given by the different researchers for helical coil heat exchanger. The analysis showed that for low Re, the graphs of $\overline{Nu}$ versus Re_t are steeper than that at high Re_t. In addition, HCTs are efficient in low Re_t. The analysis also showed that increasing δ enhances the intensity of secondary flow and consequently increases $\overline{Nu}$.

The aforementioned literature survey indicates that the majority of studies were performed on HCT with isothermal and isoflux boundary conditions or shell and coil heat exchangers with small ranges of HCT configurations and fluid operating conditions. So, the present study aims to investigate experimentally the effect of coil curvature on characteristics of convective heat transfer in horizontal shell and coil heat exchangers with same torsion over a wide range of fluid operating conditions. Present measurements were utilized to introduce experimental correlations for the average Nusselt numbers and the HCT-Fanning friction factor as a function of Reynolds number, coil curvature ratio, and Prandtl number.

2 Experimental Apparatus

The experimental facility employed in the present investigation consists of heating and cooling units, shell and coil heat exchanger, pumps, measuring devices, valves, and the connecting pipes. Figure 1 is a schematic diagram of the experimental apparatus. In addition, Fig. 2 represents photo for the present setup. Two cylindrical containers of 50 l made of stainless steel (2 mm wall thickness) were employed for hot and cold fluid tanks. Each tank was installed inside 2 mm thick galvanized steel tanks with 20 mm gap, which was injected by spray foam insulation to minimize the

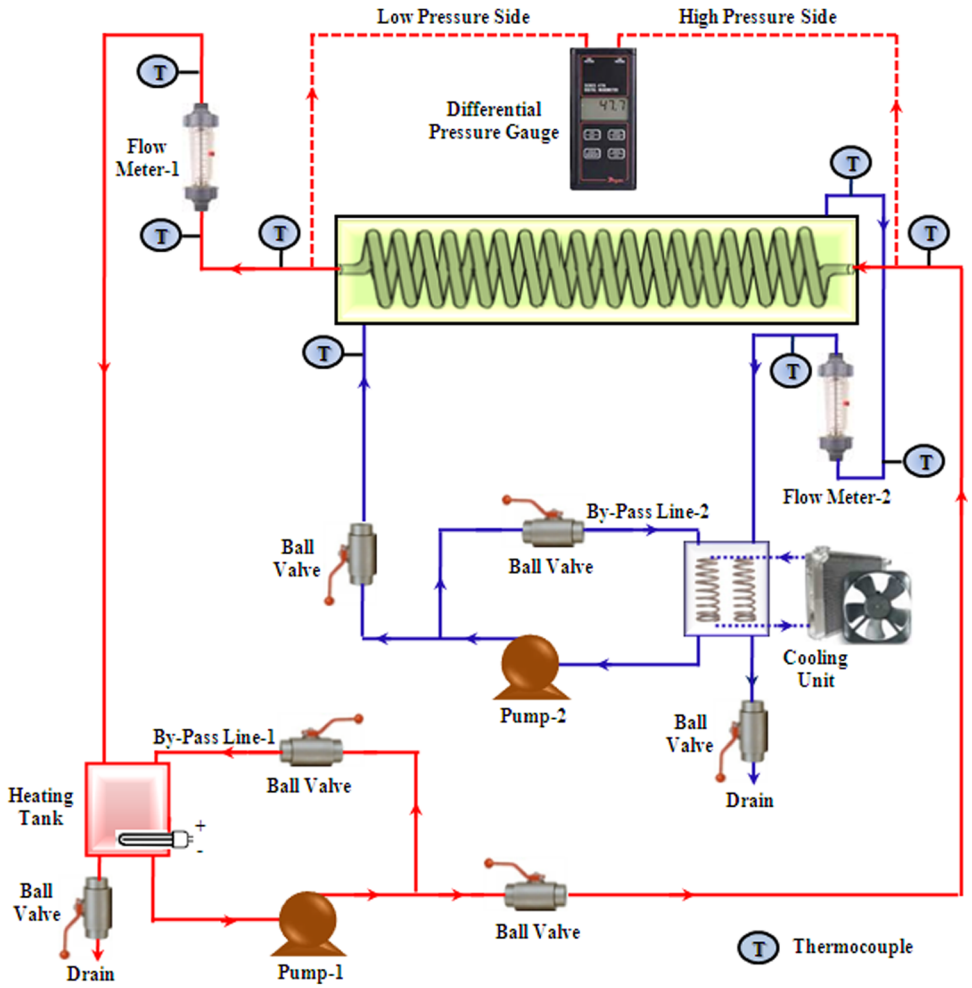

Fig. 1 Schematic diagram of the experimental apparatus

heat loss or gain. An electric heater of 6 kW rated power was fixed horizontally on the bottom of the heating tank and performed the function of heating the water to the required temperature. The heat was removed from the cooling tank by two refrigeration units of 10.5 kW cooling capacity. The electric heater and the refrigeration cooling units operate based on pre-adjusted digital thermostats, which were used to keep constant temperatures of the liquids directed to the heat exchanger.

Fig. 2 Photo for the experimental apparatus

As illustrated in Fig. 1, each circuit contains bypass line and ball valve to control the mass flow rate directed to the heat exchanger. Two identical flow meters (1.7–18 l/min) were used to measure the volume flow rates directed to the test section. Twenty eight k-type thermocouples of 0.1 mm diameter were installed within each test section to measure the temperatures. Four thermocouples were inserted into the flow streams, at approximately 60 mm from the heat exchanger ports, to measure the inlet and exit temperatures of the shell and HCT fluids.

Twenty thermocouples were used to measure the HCT wall surface temperatures. They were mounted at ten equally distanced (441.5 mm) positions on the HCT surface, with installing two thermocouples at each position on the outer and inner diameter of the coil. To achieve higher accuracy in calculation of flow rate, four thermocouples were installed at inlet and exit of flow meters to record the flow temperature. All thermocouples were connected to a digital thermometer indicator with resolution of 0.1 °C to display the thermocouples outputs. A digital differential pressure transducer was employed for measuring the pressure drop of water across the HCT. Two identical 1.5 hp rated power centrifugal pumps were installed to circulate the hot and cold water. Flexible nylon and polyvinyl chloride (PVC) tubes were used for all connections.

Five configurations shell and coil heat exchanger were constructed with different HCT curvature ratios. Due to the variation of curvature ratio ($\delta = d_{t,i}/D_c$), the coil pitch (p_c) and consequently number of turns (N) are varied to sustain constant coil torsion ratio ($\lambda = p_c/\pi D_c$) of 0.0895. The dimensions of the copper tube used in each coil are 4.415 m lengths, 9.52 mm outer diameter, and 8.3 mm inner diameter. The characteristic dimensions of

the different configurations are revealed in Table 1. A photo and schematic layout of the shell and coil heat exchanger are shown in Fig. 3.

The shell of the heat exchangers was made of mild steel (2 mm wall thickness) and was formed as cylindrical shape with the aid of rolling machine in addition to welding. Two nipples of same material and 4 mm wall thickness were welded on both ends of the shell. The distance between the nozzles centers and the neighboring shell end was 50 mm, which made the HCT partially block the opening as recommended by Kupprn [53]. Ten holes of 1 mm diameter were made in the shell wall to pass the thermocouples to their positions on the HCT surface. The holes were drilled directly facing the positions of the thermocouples to provide the smallest length of the thermocouples in the shell to minimize their effects on the shell flow. The outer surface of the shell was thermally insulated using a layer of each ceramic fiber, asbestos rope, and glass wool. Finally, all equipments were assembled: the shell and coil heat exchanger, heating and cooling units, pumps, ball valves, connecting lines, and the measuring devices.

3 Experimental Procedures and Data Reduction

The first step in collecting data from the system was to fill the heating and cooling tanks with water from the local water supply. Then, the heater, the cooling units, and the pumps were operated. Inlet temperatures of the water in both sides were adjusted by regulating the temperatures of the heating and cooling tanks through their thermostats. The flow rates were adjusted through the flow meters and the installed valves, which were regulated to obtain the required flow rates in the primary lines and the remainder is bypassed to the tanks. The range of the operating conditions is given in Table 2.

During the operation, the steady state condition is conducted when the maximum variation of 0.5 °C for each thermocouple reading is within 20 min. It should be noted that for heat transfer calculations, the fluid properties of the shell, and HCT sides were calculated at the bulk temperatures, $T_{sh,m}$ and $T_{t,m}$, respectively. While for pressure drop calculations, the HCT water properties were calculated at the film temperature, T_f, as recommended by Schmidt [33]. The bulk and film temperatures are calculated as follows:

$$T_{sh,m} = (T_{sh,i} + T_{sh,o})/2 \quad (1)$$

$$T_{t,m} = (T_{t,i} + T_{t,o})/2 \quad (2)$$

$$\bar{T}_{t,s} = \frac{\sum_{t,s}^{T}}{20} \quad (3)$$

$$T_f = (T_{m,t} + \bar{T}_{t,s})/2 \quad (4)$$

The inner surface temperature of the HCT wall was taken equal to outer surface due to very low conduction resistance of the tube wall. The water thermophysical properties were evaluated from Remsburg [54].

The measurements of the flow rates and inlet and outlet temperatures of both streams of the heat exchanger were used to calculate heat transfer rates on the HCT and shell sides (Q_t and Q_{sh}) as

$$Q_t = \dot{m}_t C_{p_t}(T_{t,i} - T_{t,o}) \quad (5)$$

(*a*)

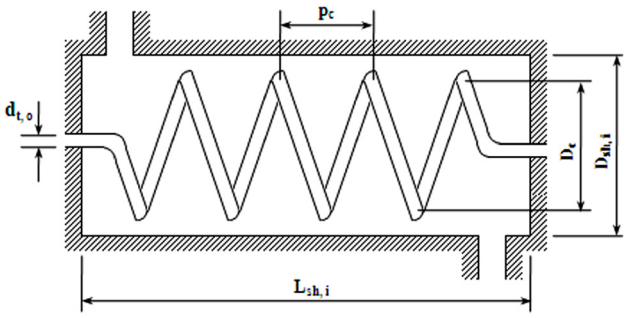

(*b*)

Fig. 3 A photo and schematic layout of the test section. (*a*) Photo of the test section (shell and coil heat exchanger). (*b*) Schematic layout of the shell and coil heat exchanger.

Table 2 Range of fluids operating conditions

HCT-side	
HCT-side water flow rate (l/min)	$1.7 - 11.158$ ($6471 \le Re_t \le 62,085$)
HCT-side inlet temperature (°C)	45, 55, 65 ($2.86 \le Pr_t \le 4.43$)
Shell-side water flow rate (l/min)	6.018
Shell-side inlet temperature (°C)	20
Shell-side	
Shell-side water flow rate (l/min)	$1.7 - 11.158$ ($179 \le Re_{sh} \le 1384$)
Shell-side inlet temperature (°C)	15, 20, 25 ($5.25 \le Pr_{sh} \le 7.54$)
HCT-side water flow rate (l/min)	6.018
HCT-side inlet temperature (°C)	55

$$Q_{sh} = \dot{m}_{sh} C_{p_{sh}}(T_{sh,o} - T_{sh,i}) \quad (6)$$

Without heat gain or loss from the heat exchanger, there is an energy balance between the two streams ($Q_t = Q_{sh}$). In the real experiments, due to measurement errors or heat gain/loss, there would always be some discrepancy between the two heat transfer rates. Therefore, the arithmetical average of the two, Q_{ave}, can be used as the heat load of the exchanger. For all experimental tests, the heating and cooling loads calculated from the hot and cold sides did not differ by more than ±1.78%

Table 1 Characteristic dimensions of the used shell and coil heat exchangers

HCT No.	D_c (mm)	δ	p_c (mm)	λ	L_c (mm)	L_{sh} (mm)	$D_{sh,i}$ (mm)	$D_{sh,h}$ (mm)	N
1	69.5	0.1194	19.52	0.0895	405	505	271	205.1	20.21
2	105.0	0.0790	29.52						13.38
3	140.5	0.0591	39.52						10
4	176.0	0.0472	49.52						7.98
5	211.5	0.0392	59.52						6.64

$$Q_{ave} = \frac{|Q_t| + |Q_{sh}|}{2} \tag{7}$$

The heat load of the heat exchanger, Q_{ave}, was used to calculate the average heat transfer coefficient for the HCT side fluid, $\bar{h}_t$, and then the average Nusselt number for the HCT side fluid, $\overline{Nu}_t$, as follows:

$$Q_{ave} = \bar{h}_t A_{t,i}\left(T_{t,m} - \bar{T}_{t,s}\right) \tag{8}$$

$$\overline{Nu}_t = \frac{\bar{h}_t\, d_{t,i}}{k_t} \tag{9}$$

The overall thermal conductance was calculated from the temperature data and flow rates using Eq. (10) as

$$U_o A_{t,o} = \frac{Q_{ave}}{\Delta T_{LM}} \tag{10}$$

$$\Delta T_{LM} = \frac{\left(T_{t,i} - T_{sh,o}\right) - \left(T_{t,o} - T_{sh,i}\right)}{\ln\left[\dfrac{T_{t,i} - T_{sh,o}}{T_{t,o} - T_{sh,i}}\right]} \tag{11}$$

Neglecting the thermal resistances of the tube wall and fouling, the overall thermal conductance can be expressed in terms of convection thermal resistances. The average heat transfer coefficient for the shell side fluid, $\bar{h}_{sh}$, and then the average Nusselt number for the shell-side fluid, $\overline{Nu}_{sh}$, can be obtained as follows:

$$\frac{1}{U_o A_{t,o}} = \frac{1}{\bar{h}_{sh} A_{t,o}} + \frac{1}{\bar{h}_t A_{t,i}} \tag{12}$$

$$\overline{Nu}_{sh} = \frac{\bar{h}_{sh}\, D_{sh,h}}{k_{sh}} \tag{13}$$

The more general definition of the hydraulic diameter of the shell side, $D_{sh,h}$, described in Shah and Sekulic [55] was used in the present work

$$D_{sh,h} = \frac{4V_f}{A_{f.c}} = \frac{4\left(V_{sh,i} - V_{t,o}\right)}{A_{f.c}} = \frac{D_{sh,i}^2 L_{sh} - d_{t,o}^2 L_t}{D_{sh,i} L_{sh} + d_{t,o} L_t} \tag{14}$$

HCT and shell Reynolds number can be written as follows:

$$Re_t = \frac{4\dot{m}_t}{\pi d_{t,i} \mu_t} \tag{15}$$

$$Re_{sh} = \frac{4\dot{m}_{sh}}{\pi D_{sh,h} \mu_{sh}} \tag{16}$$

The Fanning friction factor for the fluid in circulation inside the HCT, f_c, was calculated with the following equation:

$$f_c = \frac{\Delta P_c\, d_{t,i}}{2 L_t\, \rho_t u^2} = \frac{\Delta P_c\, \pi^2\, \rho_t\, d_{t,i}^5}{32\, L_t\, \dot{m}_t^2} \tag{17}$$

Daily and Harleman [56] reported that the developed region in HCTs may be along a distance equal to 50 diameters of the HCT. Also, Nigam et al. [57] presented that the fully developed region in HCTs is formed after a distance equal to 30 diameters of the HCT. These values represent 5.64–9.4% of the total length of the HCTs used in the present study, which can be neglected and the fully developed profiles are confirmed.

4 Uncertainty Analyses

In general, the accuracy of the experimental results depends on the accuracy of the individual measuring instruments and techniques. It should be noted that according to the manufacturer, uncertainty (ω) in the HCT outer and inner diameters is ± 0.01 mm, which can be neglected. The uncertainty in the measured coil and shell dimensions was assumed to be ± 0.5 mm; this was guessed quantity from meter scale. In addition, the uncertainty applied to the thermal properties of water was assumed to be $\pm 0.1\%$. The uncertainty is calculated based upon the root sum square combination of the effects of each of the individual inputs as introduced by Kline and McClintock [58]. For all experimental runs, the uncertainty in Re_t and Re_{sh} was $\pm 1.67\%$. Also, the average uncertainty was $\pm 4.96\%$ in $\overline{Nu}_t$, $\pm 2.57\%$ in $\overline{Nu}_{sh}$, $\pm 2.16\%$ in U_o, and $\pm 3.66\%$ in f_c.

5 Results and Discussion

First, the experimental apparatus and procedures were validated by comparing the results of $\overline{Nu}_t$ for water flowing through the HCT with $\overline{Nu}_t$ reported from literature. From the literature review, it is obvious that there is lack in the correlations required to calculate the heat transfer coefficient for applied shell and coil heat exchangers. On the contrary, there are a number of correlations in the literature for the $\overline{Nu}_t$ for water flowing through the HCT with isoflux and isothermal wall boundary conditions.

Here, the present experimental data for $\overline{Nu}_t$ were validated with the experimental data obtained by Xin and Ebadian [43], and Rogers and Mayhew [39] as they were used by Purandare et al. [52]. In addition, another comparison of the experimental data for HCT-Fanning friction factor with the results of White [28] and Prasad et al. [34] was performed. The results of these comparisons are shown in Fig. 4. From this figure, it can be seen that the experimental results for both heat transfer and friction factor calculations are in good agreement with previous studies.

A series of 295 experiments were carried out on five heat exchangers shown in Table 1, which were constructed with different coil curvature ratios. These configurations were tested at different mass flow rates and inlet temperatures for the two sides of heat exchanger as presented in Table 2. The corresponding dimensionless parameters are $6471 \le Re_t \le 62085$, $2.86 \le Pr_t \le 4.43$, $1329 \le De_t \le 20927$, $179 \le Re_{sh} \le 1384$, $5.25 \le Pr_{sh} \le 7.54$, and $0.0392 \le \delta \le 0.1194$.

5.1 Heat Transfer Results. Results of heat transfer in terms of HCT and shell Nusselt numbers are presented for the different governing parameters. First, the operating conditions are hold constant in the shell side at $T_{sh,i} = 20\,^{\circ}C$ and $\dot{V}_{sh} = 6.018\,l/min$, while the HCT operating conditions are varied according to

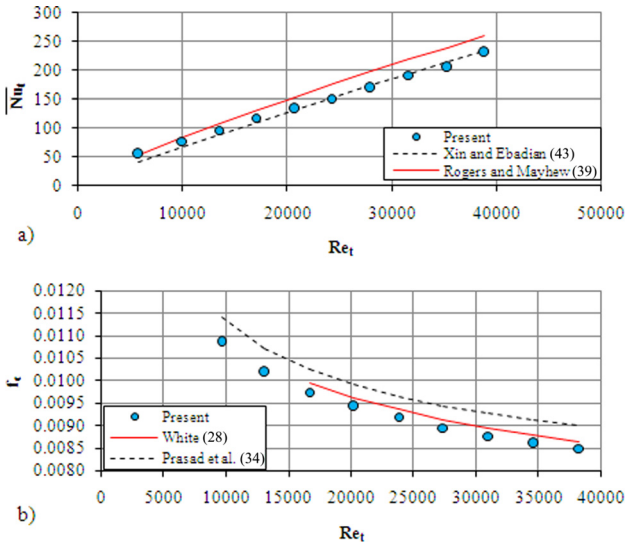

Fig. 4 Validation of the experimental data for HCT ($\delta = 0.0591$)

Table 2. Figure 5 illustrates the effect of coil curvature ratio on HCT average Nusselt number versus HCT Reynolds number for $0.0392 \leq \delta \leq 0.1194$ at $T_{t,i} = 55\,^{\circ}C$.

From Fig. 5, it is clear that increasing coil curvature ratio increases HCT-average Nusselt number. The average increase in the HCT-average Nusselt number is of 160.3–80.6%, and the average increase in the overall heat transfer coefficient is of 116.9–110.8% when the coil curvature ratio increases from 0.0392 to 0.1194 for $6471 \leq Re_t \leq 62085$. This can be attributed to increasing the centrifugal force with higher coil curvature ratio, which induces more effective secondary flow. Also, it is clear that increasing HCT-Reynolds number increases the HCT-average Nusselt number at the same coil curvature ratio. This can be returned to the effective secondary flow due to centrifugal force, which increases at higher Reynolds number.

The thermal performance of the shell side is introduced for $179 \leq Re_{sh} \leq 1384$, $5.25 \leq Pr_{sh} \leq 7.54$, and $0.0392 \leq \delta \leq 0.1194$. The inlet flow rate and temperature at HCT fluid remain constant at 6.018 l/min and 55 °C, respectively. Figure 6 shows the shell average Nusselt number versus shell side Reynolds number at $T_{sh,i} = 20\,^{\circ}C$.

From Fig. 6, it is clear that increasing coil curvature ratio leads to increase $\overline{Nu}_{sh}$ even at same Re_{sh}. The average increase is of 224.3–92.6% in shell Nusselt number and 210.8–93.2% in the overall heat transfer coefficient when the coil curvature ratio increases from 0.0392 to 0.1194 for $179 \leq Re_{sh} \leq 1384$. This is because of increasing number of HCT turns and decreasing coil pitch associated with increasing δ provides more sequential fluid impingement with the coil surface, and consequently enhances $\overline{Nu}_{sh}$ and U_o. Also, it is clear that increasing Re_{sh} increases $\overline{Nu}_{sh}$ and U_o at same δ and $T_{sh,i}$. This can be attributed to increasing the fluctuations and fluid layers mixing around the coil turns by increasing Re_{sh}.

The influence of the coil form (p_c and N) with the same tube length and the same coil torsion on the HCT average Nusselt number and the overall heat transfer coefficient for the five configurations at $T_{t,i} = 55\,^{\circ}C$, $T_{sh,i} = 20\,^{\circ}C$ and $\dot{V}_{sh} = 6.018$ l/min are shown in Figs. 7 and 8. The results are presented as a function of Dean number ($De_t = Re_t\,\delta^{0.5}$) instead of Re_t to compare the obtained values of $\overline{Nu}_t$ and U_o at the same centrifugal force inside the HCT.

From Fig. 7, it is clear that the effect of coil form (p_c and N) on HCT average Nusselt number is almost insignificant for a specific De_t. This can be returned to the same fabricated coil ratio and the same driving centrifugal force inside HCT for a specific Dean number. However, the coil form effect on the overall heat transfer coefficient is noticeable at the same De_t with shell flow rate remains constant as shown in Fig. 8. This can be attributed to higher turns number and small pitch provides more turbulence level as a result of sequential fluid impingement on the external surface of the coil which enhances shell side convection heat coefficient and consequentially the overall heat transfer coefficient.

The influence of coil and shell inlet temperatures on the thermal performance of the heat exchanger ($\overline{Nu}_t$ and $\overline{Nu}_{sh}$) is studied for $0.0392 \leq \delta \leq 0.1194$. The influence of fluid inlet temperature inside coil on the HCT average Nusselt number at $\delta = 0.0591$ is shown in Fig. 9. The experimental runs were performed for coil inlet fluid temperature at $T_{ti} = 45$, 55 and 65 °C corresponding to $2.86 \leq Pr_t \leq 4.43$.

The effect of shell fluid inlet temperature at $\delta = 0.0591$, $T_{sh,i} = 15$, 20, and 25 °C is shown in Fig. 10.

For all tested heat exchangers, it is clear that as the inlet temperature at both sides increases, $\overline{Nu}_t$ and $\overline{Nu}_{sh}$ decrease at same Reynolds number. This can be attributed to the decrease in Prandtl number with increasing the fluid temperature.

5.2 HCT Friction Factor. Experimental runs were carried out to study the effects of coil curvature and HCT fluid inlet temperature on friction factor inside HCT. The mass flow rate is varied from 1.7 to 11.158 l/min and coil inlet fluid temperature of

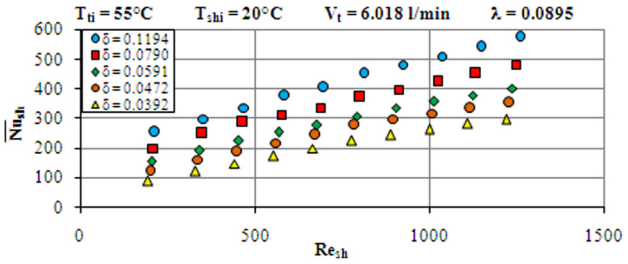

Fig. 6 Variation of shell Nusselt number with shell-side Reynolds number at different HCT-curvature ratios

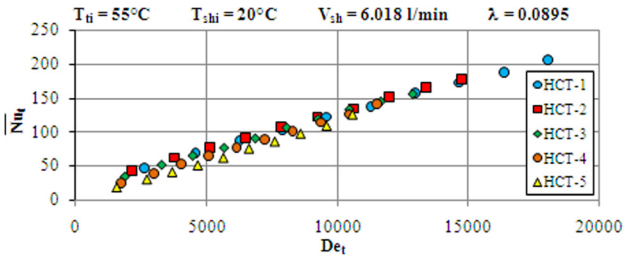

Fig. 7 Variation of coiled tube Nusselt number with HCT-side Dean number at different HCTs

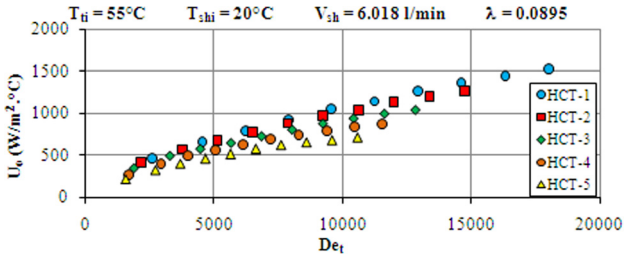

Fig. 8 Variation of overall heat transfer coefficient with HCT-side Dean number at different HCTs

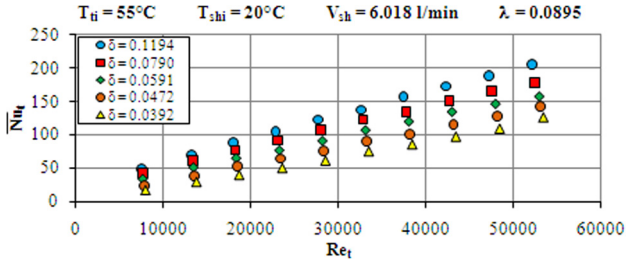

Fig. 5 HCT average Nusselt number versus HCT Reynolds number at different coil curvature ratios

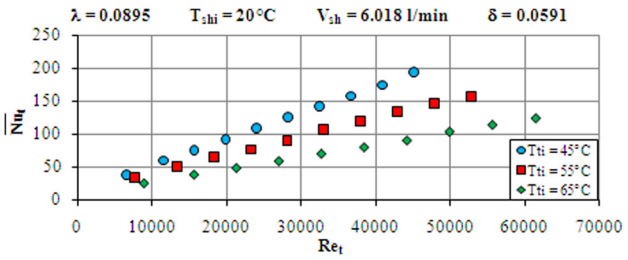

Fig. 9 Average HCT Nusselt number versus Reynolds number at different HCT-inlet temperatures

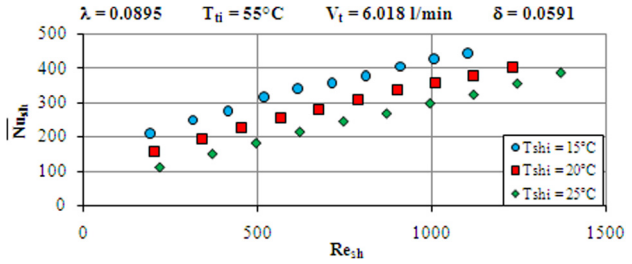

Fig. 10 Shell Nusselt number versus shell Reynolds number at different shell inlet temperatures

$T_{ti} = 45$, 55, and 65 °C. The corresponding dimensionless parameters are $6389 \leq \mathrm{Re_t} \leq 60,227$ and $0.0392 \leq \delta \leq 0.1194$. Figure 11 presents the effect of coil curvature ratio for three different inlet temperatures at $T_{sh,i} = 20$ °C and $\dot{V}_{sh} = 6.018$l/min.

From Fig. 11, it is seen that Fanning friction factor increases noticeably when coil curvature ratio increases at the same $\mathrm{Re_t}$. The average increase in HCT-friction factor is of 33.2–7.7% when the coil curvature ratio increases from 0.0392 to 0.1194. This can be attributed to the higher centrifugal force that induces more secondary flow and consequentially the friction factor inside the HCT.

Figure 12 shows the effect of HCT fluid inlet temperature on the Fanning friction factor at $\delta = 0.1194$ and 0.0392. It is clear that the effect of $T_{t,i}$ on f_c is nearly insignificant especially at higher Ret. This may be returned to the low effect of viscous force compared with the higher centrifugal force, which is the dominant at HCT Reynolds number.

6 Correlations for Average Nusselt Numbers and Fanning Friction Factor

Using the present experimental data, correlations were developed to predict the average Nusselt number of both sides of shell and coil heat exchanger and the Fanning friction factor inside the HCT.

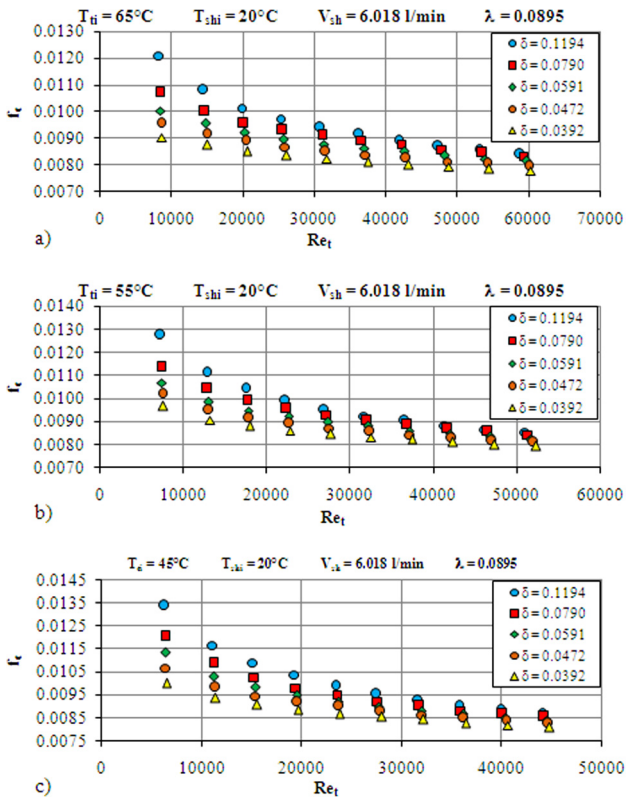

Fig. 11 Variation of HCT-Fanning friction factor with HCT-side Reynolds number at different HCT-curvature ratios: (*a*) $T_{ti} = 65$ °C, (*b*) $T_{ti} = 55$ °C, and (*c*) $T_{ti} = 45$ °C

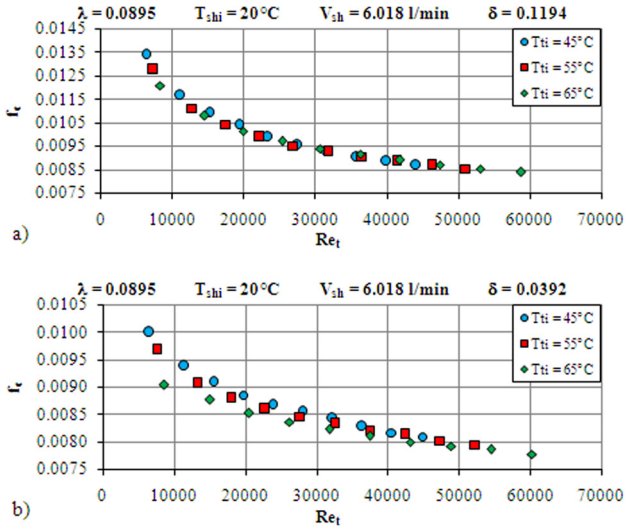

Fig. 12 Effect of HCT inlet temperature on the HCT Fanning friction factor: (a) $\delta = 0.1194$ and (b) $\delta = 0.0392$

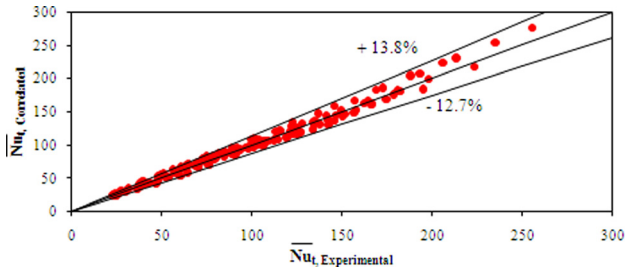

Fig. 13 Comparison of experimental values for HCT average Nusselt number with that correlated by Eq. (18)

The HCT average Nusselt number is correlated as a function of HCT Reynolds and Prandtl numbers and coil curvature ratio

$$\overline{\mathrm{Nu}}_t = 0.00241\,\mathrm{Re}^{0.9293}\,\mathrm{Pr}^{2.0177}\,\delta^{0.556} \tag{18}$$

Equation (18) is applicable for $6471 \leq \mathrm{Re_t} \leq 62,085$, $2.86 \leq \mathrm{Pr_t} \leq 4.43$, $1329 \leq \mathrm{De_t} \leq 20,927$, and $0.0392 \leq \delta \leq 0.1194$ with maximum deviation of 13.8%.

From the test runs that were performed for the shell-side, a correlation to estimate $\overline{\mathrm{Nu}}_{sh}$ was obtained as follows:

$$\overline{\mathrm{Nu}}_{sh} = 4.4275\,\mathrm{Re}^{0.4922}\,\mathrm{Pr}^{1.5676}\,\delta^{0.6964} \tag{19}$$

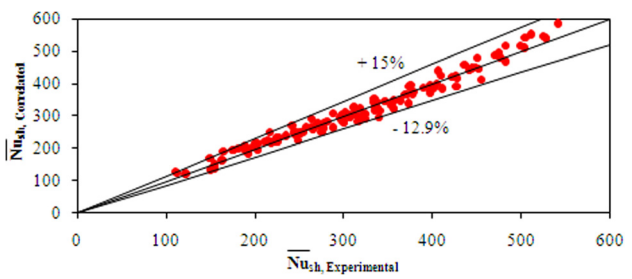

Fig. 14 Comparison of experimental values for shell average Nusselt number with that correlated by Eq. (19)

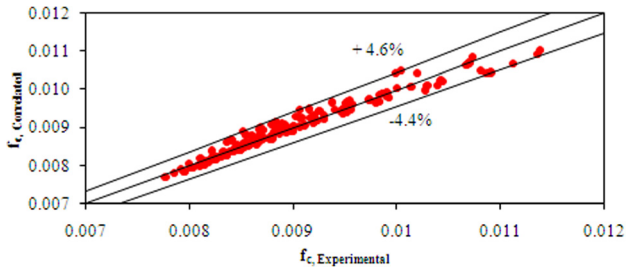

Fig. 15 Comparison of experimental values for coiled tube-Fanning friction factor with that correlated by Eq. (20)

Equation (19) is applicable for $179 \leq \mathrm{Re_{sh}} \leq 1384$, $5.25 \leq \mathrm{Pr_{sh}} \leq 7.54$, and $0.0392 \leq \delta \leq 0.1194$ with maximum deviation of 15%.

Additionally, a correlation for Fanning friction factor in the HCT was obtained within $6389 \leq \mathrm{Re_t} \leq 60,227$, $1286 \leq \mathrm{De_t} \leq 20,284$, and $0.0392 \leq \delta \leq 0.1194$ with maximum deviation 4.6%

$$f_c = 0.04883\,\mathrm{Re}^{-0.1372}\ \delta^{0.105} \tag{20}$$

From these figures, it is evident that the proposed correlations are in good agreement with the present experimental data (Figs. 13–15).

7 Conclusions

The present work was carried out to investigate the heat transfer characteristics in shell and coil heat exchanger, in addition to the pressure drop inside the HCTs. The influence of coil curvature and HCT and shell Reynolds numbers for the same coil torsion were discussed. The investigated ranges are $6471 \leq \mathrm{Re_t} \leq 62,085$, $2.86 \leq \mathrm{Pr_t} \leq 4.43$, $1329 \leq \mathrm{De_t} \leq 20,927$, $179 \leq \mathrm{Re_{sh}} \leq 1384$, $5.25 \leq \mathrm{Pr_{sh}} \leq 7.54$, and $0.0392 \leq \delta \leq 0.1194$. From the study, it could be concluded that

- The average Nusselt numbers of the two sides of the heat exchangers and the overall heat transfer coefficients increase with increasing coil curvature ratio. The average increase is 160.3–80.6% for HCT average Nusselt number and 224.3–92.6% for shell average Nusselt number when the coil curvature ratio increases from 0.0392 to 0.1194.
- For the same flow rate in both heat exchanger sides, the effect of coil pitch and number of turns with the same coil torsion and tube length is remarkable on shell average Nusselt number while it is insignificant on HCT average Nusselt number.
- Fanning friction factor in the HCTs significantly increases with increasing coil curvature. The average increase in HCT friction factor is of 33.2–7.7% when the coil curvature ratio increases from 0.0392 to 0.1194. Also, the effect of HCT inlet temperature on the Fanning friction factor is nearly insignificant especially at higher HCT Reynolds number.
- Correlations for the average Nusselt numbers of the two sides of shell and coil heat exchanger and the HCT Fanning friction factor as a function of the investigated parameters were obtained.

Nomenclature

A = area (m^2)
C_p = specific heat (J/kg °C)
d = diameter (m)
D = diameter (m)
f = fanning friction factor
h = average convection heat transfer coefficient ($\mathrm{W/m^2\,°C}$)
k = thermal conductivity ($\mathrm{W/m^2\,°C}$)
L = length (m)
$\dot{m}$ = mass flow rate (kg/s)
N = number of turns of the HCT
p = pitch of the HCT (m)
P = pressure (Pa)
Q = heat transfer rate (W)
S = spacing of HCT (m)
T = temperature (°C)
u = mean axial velocity (m/s)
U = overall heat transfer coefficient ($\mathrm{W/m^2\,°C}$)
V = volume (m^3)

Greek Symbols

δ = dimensionless coil curvature ratio ($d_{t,i}/D_c$)
λ = dimensionless pitch ratio (coil torsion) ($p_c/\pi D_c$)
μ = dynamic viscosity (kg/m s)
π = Pi ≡ a mathematical constant ≅ 3.1416
ρ = density ($\mathrm{kg/m}^3$)
ω = uncertainty

Superscripts and Subscripts

ave = average
c = coil/contact
f = film/fluid/core flow
h = hydraulic
i = inner/inlet/internal
LM = logarithmic mean
m = mean
o = out/outer
s = surface
sh = shell
t = tube

Dimensionless Groups

De = Dean number ($\mathrm{Re}\,\delta^{0.5}$)
$\overline{\mathrm{Nu}}$ = average Nusselt number
Pr = Prandtl number
Re = Reynolds number

Acronyms and Abbreviations

HCT = helically coiled tube
PVC = polyvinyl chloride

References

[1] Abu-Mulaweh, H. I., 2003, "Experimental Comparison Between Heat Transfer Enhancement Methods in Heat Exchangers," Int. J. Mech. Eng. Educ., **31**(2), pp. 160–167.
[2] Berger, S. A., Talbot, L., and Yao, L. S., 1983, "Flow in Curved Pipes," Annu. Rev. Fluid Mech., **15**, pp. 461–512.
[3] Abdalla, M. A., 1994, "A Four-Region, Moving-Boundary Model of a Once Through, Helical-Coil Steam Generator," Ann. Nucl. Energy, **21**(9), pp. 541–562.
[4] Rao, B. K., 1994, "Turbulent Heat Transfer to Power-Law Fluids in Helical Passages," Int. J. Heat Fluid Flow, **15**(2), pp. 142–148.
[5] Rabin, Y., and Korin, E., 1996, "Thermal Analysis of a Helical Heat Exchanger for Ground Thermal Energy Storage in Arid Zones," Int. J. Heat Mass Transfer, **39**(5), pp. 1051–1065.
[6] Bai, B., Guo, L., Feng, Z., and Chen, X., 1999, "Turbulent Heat Transfer in a Horizontally Coiled Tube," Heat Transfer Asian Res., **28**(5), pp. 395–403.
[7] Sandeep, K. P., and Palazoglu, T. K., "Secondary Flow in Coiled Tubes," ASAE Annual International Meeting, Paper No. 996148.
[8] Genssle, A., and Stephan, K., 2000, "Analysis of the Process Characteristics of an Absorption Heat Transformer With Compact Heat Exchangers and the Mixture TFE-E181," Int. J. Therm. Sci., **39**(1), pp. 30–38.
[9] Kern, D. Q., 2000, *Process Heat Transfer*, Tata McGraw-Hill, 4th reprint, pp. 37–57.
[10] Rennie, T. J., 2004, *Numerical and Experimental Studies of a Double-Pipe Helical Heat Exchanger*, Department of Bioresource Engineering, McGill University, Montreal, Canada.

[11] Kumar, V., Saini, S., Sharma, M., and Nigam, K. D. P., 2006, "Pressure Drop and Heat Transfer Study in Tube-in-Tube Helical Heat Exchanger," Chem. Eng. Sci., **61**(13), pp. 4403–4416.
[12] Chingulpitak, S., and Wongwises, S., 2010, "Effects of Coil Diameter and Pitch on the Flow Characteristics of Alternative Refrigerants Flowing Through Adiabatic Helical Capillary Tubes," Int. Commun. Heat Mass Transfer, **37**(9), pp. 1305–1311.
[13] Chingulpitak, S., and Wongwises, S., 2011, "A Comparison of Flow Characteristics of Refrigerants Flowing Through Adiabatic Straight and Helical Capillary Tubes," Int. Commun. Heat Mass Transfer, **38**(3), pp. 398–404.
[14] Huminic, G., and Huminic, A., 2011, "Heat Transfer Characteristics in Double Tube Helical Heat Exchangers Using Nanofluids," Int. J. Heat Mass Transfer, **54**(19–20), pp. 4280–4287.
[15] Zhao, Z., Wang, X., Che, D., and Cao, Z., 2011, "Numerical Studies on Flow and Heat Transfer in Membrane Helical-Coil Heat Exchanger and Membrane Serpentine-Tube Heat Exchanger," Int. Commun. Heat Mass Transfer, **38**(9), pp. 1189–1194.
[16] Pimenta, T. A., and Campos, J. B. L. M., 2012, "Friction Losses of Newtonian and Non-Newtonian Fluids Flowing in Laminar Regime in a Helical Coil," Exp. Therm. Fluid Sci., **36**, pp. 194–204.
[17] Topakoglu, H. C., 1967, "Steady Laminar Flows of an Incompressible Viscous Fluid in Curved Pipes," J. Math. Mech., **16**(12), pp. 1321–1337.
[18] McConalogue, D. J., and Srivastava, R. S., 1968, "Motion of a Fluid in a Curved Tube," Proc. R. Soc. London, Ser. A, Math. Phys. Sci., **307**(1488), pp. 37–53.
[19] Hüttl, T. J., and Friedrich, R., 2000, "Influence of Curvature and Torsion on Turbulent Flow in Helically Coiled Pipes," Int. J. Heat Fluid Flow, **21**(3), pp. 345–353.
[20] Hüttl, T. J., and Friedrich, R., 2001, "Direct Numerical Simulation of Turbulent Flows in Curved and Helically Coiled Pipes," Comput. Fluids, **30**(5), pp. 591–605.
[21] Gammack, D., and Hydon, P. E., 2001, "Flow in Pipes With Non-Uniform Curvature and Torsion," J. Fluid Mech., **433**, pp. 357–382.
[22] Masud, M. A., Rabiul Islam, Md., Rasel Sheikh, Md., and Alam, Md. M., 2010, "Stable Solution Zone for Fluid Flow Through Curved Pipe With Circular Cross-Section," J. Naval Archit. Mar. Eng., **7**(1), pp. 19–26.
[23] Yu, B., Zheng, B., Lin, C. X., Pena, O. J., and Ebadian, M. A., 2003, "Laser Doppler Anemometry Measurements of Laminar Flow in Helical Pipes," Exp. Therm. Fluid Sci., **27**(8), pp. 855–865.
[24] Eustice, J., 1910, "Flow of Water in Curved Pipes," Proc. R. Soc. London, Ser. A, **84**, pp. 107–118.
[25] Eustice, J., 1911, "Experiments of Streamline Motion in Curved Pipes," Proc. R. Soc. London, Ser. A, **85**(576), pp. 119–131.
[26] Dean, W. R., 1928, "The Streamline Motion of Fluid in a Curved Pipe," Philos. Mag. J. Sci., Series, **7**(5), pp. 673–695.
[27] White, C. M., 1929, "Streamline Flow Through Curved Pipes," Proc. R. Soc. London, Ser. A, **123**(792), pp. 645–663.
[28] White, C. M., 1932, "Friction Factor and its Relation to Heat Transfer," Trans. Inst. Chem. Eng., **18**, pp. 66–86.
[29] Ito, H., 1959, "Friction Factors for Turbulent Flow in Curved Pipes," ASME J. Basic Eng., **81**, pp. 123–134.
[30] Mori, Y., and Nakayama, W., 1965, "Study on Forced Convection Heat Transfer in Curved Pipes, 1st Report, Laminar Region," Int. J. Heat Mass Transfer, **8**(1), pp. 67–82.
[31] Mori, Y., and Nakayama, W., 1967, "Study on Forced Convective Heat Transfer in Curved Pipes, 2nd Report, Turbulent Region," Int. J. Heat Mass Transfer, **10**(1), pp. 37–59.
[32] Mori, Y., and Nakayama, W., 1967, "Study on Forced Convective Heat Transfer in Curved Pipes, 3rd Report, Theoretical Analysis Under the Condition of Uniform Wall Temperature and Practical Formula," Int. J. Heat Mass Transfer, **10**(5), pp. 681–695.
[33] Schmidt, E. F., 1967, "Heat Transfer and Pressure Loss in Spiral Tubes," Chem. Eng. Tech., **39**, pp. 781–789.
[34] Prasad, B., Das, D. H., and Prabhakar, A. K., 1989, "Pressure Drop, Heat Transfer and Performance of a Helical Coil Tubular Exchanger," J. Heat Recovery Combined Heat Power, **9**(3), pp. 249–256.
[35] Ali, S., 2001, "Pressure Drop Correlations for Flow through Regular Helical Coil Tubes," Fluid Dyn. Res., **28**(4), pp. 295–310.
[36] Pimenta, T. A., and Campos, J. B., 2012, "Friction Losses of Newtonian and Non-Newtonian Fluids Flowing in Laminar Regime in a Helical Coil," Exp. Therm. Fluid Sci., **36**, pp. 194–204.
[37] Kirpikov, A. V., 1957, "Heat Transfer in Helically Coiled Pipes," Trudi. Moscov. Inst. Khim. Mashinojtrojenija, **12**, pp. 43–56.
[38] Seban, R. A., and McLaughlin, E. F., 1963, "Heat Transfer in Tube Coils With Laminar and Turbulent Flow," Int. J. Heat Mass Transfer, **6**(5), pp. 387–395.
[39] Rogers, G. F., and Mayhew, Y. R., 1964, "Heat Transfer and Pressure Loss in Helically Coiled Tubes With Turbulent Flow," Int. J. Heat Mass Transfer, **7**(11), pp. 1207–1216.
[40] Kalb, C. E., and Seader, J. D., 1972, "Heat and Mass Transfer Phenomena for Viscous Flow in Curved Circular Tubes," Int. J. Heat Mass Transfer, **15**(4), pp. 801–817.
[41] Janssen, L. A., and Hoogendoorn, C. J., 1978, "Laminar Convective Heat Transfer in Helical Coiled Tubes," Int. J. Heat Mass Transfer, **21**(9), pp. 1197–1206.
[42] Zapryanov, Z., Christov, C., and Toshev, E., 1980, "Fully Developed Laminar Flow and Heat Transfer in Curved Tubes," Int. J. Heat Mass Transfer, **23**(6), pp. 873–880.
[43] Xin, R. C., and Ebadian, M. A., 1997, "The Effects of Prandtl Numbers on Local and Average Convective Heat Transfer Characteristic in Helical Pipes," ASME J. Heat Transfer, **119**(3), pp. 467–473.
[44] Prabhanjan, D. G., Raghavan, G. S., and Rennie, T. J., 2002, "Comparison of Heat Transfer Rates Between a Straight Tube Heat Exchanger and a Helically Coiled Heat Exchanger," Int. Commun. Heat Mass Transfer, **29**(2), pp. 185–191.
[45] Rennie, T. J., and Raghavan, V. G., 2005, "Experimental Studies of a Double-Pipe Helical Heat Exchanger," Exp. Therm. Fluid Sci., **29**(8), pp. 919–924.
[46] Rennie, T. J., and Raghavan, V. G., 2006, "Numerical Studies of a Double-Pipe Helical Heat Exchanger," Appl. Therm. Eng., **26**(11–12), pp. 1266–1273.
[47] Jayakumar, J. S., Mahajani, S. M., Mandal, J. C., Vijayan, P. K., and Bhoi, R., 2008, "Experimental and CFD Estimation of Heat Transfer in Helically Coiled Heat Exchangers," Chem. Eng. Res. Des., **86**(3), pp. 221–232.
[48] Jayakumar, J. S., Mahajani, S. M., Mandal, J. C., Iyer, K. N., and Vijayan, P. K., 2010, "CFD Analysis of Single-Phase Flows Inside Helically Coiled Tubes," Comput. Chem. Eng., **34**(4), pp. 430–446.
[49] Shokouhmand, H., Salimpour, M. R., and Akhavan-Behabadi, M. A., 2008, "Experimental Investigation of Shell and Coiled Tube Heat Exchangers Using Wilson Plots," Int. Commun. Heat Mass Transfer, **35**(1), pp. 84–92.
[50] Salimpour, M. R., 2008, "Heat Transfer Characteristics of a Temperature-Dependent-Property Fluid in Shell and Coiled Tube Heat Exchangers," Int. Commun. Heat Mass Transfer, **35**(9), pp. 1190–1195.
[51] Salimpour, M. R., 2009, "Heat Transfer Coefficients of Shell and Coiled Tube Heat Exchangers," Exp. Therm. Fluid Sci., **33**(2), pp. 203–207.
[52] Purandare, P. S., Lele, M. M., and Gupta, R., 2012, "Parametric Analysis of Helical Coil Heat Exchanger," ASME Int. J. Eng. Res. Technol., **1**(8), pp. 1–5.
[53] Kupprn, T., 2000, *Heat Exchanger Design Handbook*, Marcel Dekker, Inc, New York.
[54] Remsburg, R., 2001, *Thermal Design of Electronic Equipment, Electronics Handbook Series*, CRC Press Boca Raton, FL.
[55] Shah, R. K., and Sekulic, D. P., 2003, *Fundamentals of Heat Exchanger Design*, Wiley, New York.
[56] Daily, J. W., and Harleman, D. R. F., 1966, *Fluid Dynamics*, Addison Wesley, Don MiIls, Ontario, Canada.
[57] Nigam, K. D. P., Agarwal, S., and Srivastava, V. K., 2001, "Laminar Convection of Non-Newtonian Fluids in the Thermal Entrance Region of Coiled Circular Tubes," Chem. Eng. J., **84**(3), pp. 223–237.
[58] Kline, S. J., and McClintock, F. A., 1953, "Describing Uncertainties in Single-Sample Experiments," Mech. Eng., **75**(1), pp. 3–8.